

# Scaling and Universality at Ramped Quench Dynamical Quantum Phase Transitions

Sara Zamani,<sup>1</sup> J. Naji,<sup>2</sup> R. Jafari,<sup>1,3,4,\*</sup> and A. Langari<sup>5,†</sup>

<sup>1</sup>*Department of Physics, Institute for Advanced Studies in Basic Sciences (IASBS), Zanjan 45137-66731, Iran*

<sup>2</sup>*Department of Physics, Faculty of Science, Ilam University, Ilam, Iran*

<sup>3</sup>*School of Nano Science, Institute for Research in Fundamental Sciences (IPM), 19395-5531, Tehran, Iran*

<sup>4</sup>*Department of Physics, University of Gothenburg, SE 412 96 Gothenburg, Sweden*

<sup>5</sup>*Department of Physics, Sharif University of Technology, P.O.Box 11155-9161, Tehran, Iran*

The nonequilibrium dynamics of a periodically driven extended XY model, in the presence of linear time dependent magnetic field, is investigated using the notion of dynamical quantum phase transitions (DQPTs). Along the similar lines to the equilibrium phase transition, the main purpose of this work is to search the fundamental concepts such as scaling and universality at the ramped quench DQPTs. We have shown that the critical points of the model, where the gap closing occurs, can be moved by tuning the driven frequency and consequently the presence/absence of DQPTs can be flexibly controlled by adjusting the driven frequency. We have uncovered that, for a ramp across the single quantum critical point, the critical mode at which DQPTs occur is classified into three regions: the Kibble-Zurek (KZ) region, where the critical mode scales linearly with the square root of the sweep velocity, pre-saturated (PS) region, and the saturated (S) region where the critical mode makes a plateau versus the sweep velocity. While for a ramp that crosses two critical points, the critical modes disclose just KZ and PS regions. On the basis of numerical simulations, we find that the dynamical free energy scales linearly with time, as approaches to DQPT time, with the exponent  $\nu = 1 \pm 0.01$  for all sweep velocities and driven frequencies.

## I. INTRODUCTION

In the recent decades remarkable attention has focused on studying the out-of-equilibrium physics of low dimensional quantum systems [1–7]. The renaissance of the topic was commenced by the experimental advances achieved with ultra-cold atoms in optical lattices [8–11] which made possible to prepare and control non-equilibrium states with previously unexpected controllability and stability [12]. Thereafter, trapped ions [13–15], nitrogen-vacancy centres in diamond [16], superconducting qubit systems [17] and quantum walks in photonic systems [18, 19] developed to provide a framework for studying experimentally a wide variety of non-equilibrium systems. These experiments have also provoked huge progress in theoretical physics.

Recently, new research direction of quantum phase transition proposed theoretically in nonequilibrium quantum systems, titled dynamical quantum phase transitions (DQPTs) [20, 21] as a counterpart of equilibrium phase transitions. The concept of DQPT emanates from the analogy between the equilibrium partition function of a system, and Loschmidt amplitude, which measures the overlap between an initial state and its time-evolved one [20–40]. As the equilibrium phase transition is signaled by non-analyticities in the thermal free energy, the DQPT is revealed through the nonanalytical behavior of dynamical free energy, where the real-time plays the role of the control parameter [41–60]. DQPT displays a phase transition between dynamically emerging quantum phases, that takes place during the nonequilibrium coherent quantum time evolution under sudden/ramped quench [61–78, 81–86] or time-periodic modulation of Hamiltonian [16, 87–93]. In addition, a dynamical topological order parameter (DTOP) has been proposed to capture DQPTs [94, 96], analogous to order parameters at equilibrium quantum phase transition. DTOP reveals integer values as a function of time and its unit magnitude jumps, at the dynamical phase transition times, manifest the topological distinctive feature of DQPTs [97–99]. Just a while ago, DQPT was observed experimentally in several studies [11, 13, 14, 17, 18, 100–103] to confirm theoretical anticipation. Most of these researches associated with quantum evolution generated by a sudden quench of the Hamiltonian. However, comparatively little attention has been devoted to the more realistically driving systems, ramp quench, and specifically, the scaling and universality at ramped quench DQPTs. Understanding the scaling and universality at ramped quench DQPTs is of utmost importance both in designing experiments and comprehend the results [104, 105]. In this paper, we try to contribute to understand the scaling and universality of the non-equilibrium properties of the model using the notion of the DQPTs. Using the advantage of controlling the location of the equilibrium phase transition points by driven frequency, we

---

\* jafari@iasbs.ac.ir, raadmehr.jafari@gmail.com

† langari@sharif.edu

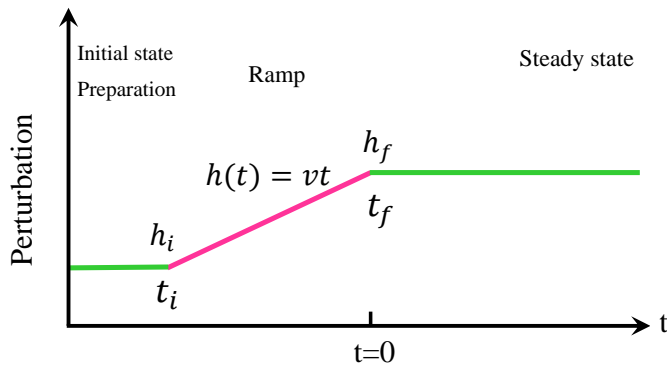


FIG. 1. (Color online) Illustration of a linear ramped quench (pink color). Here  $h(t)$  is the magnetic field,  $h_i$  and  $h_f$  its initial and final values, and  $t_i$  and  $t_f = 0$  the corresponding times.

numerically show that the behaviour of the critical momentum at which the DQPTs occur can be categorized into three distinct regions versus the sweep velocity. Moreover, we find that the dynamical free energy close to DQPT time shows a power law scaling with the exponent  $\nu = 1 \pm 0.01$ , for any sweep velocities which is the same as that of the sudden quench.

The paper is organized as follows. In Sec. II, the dynamical free energy and DQPT of the two band Hamiltonians are discussed. In Sec. III we present the model and review its exact solution and equilibrium phase transition. Section IV is dedicated to the numerical simulation of the model based on the analytical result. Section V contains some concluding remarks.

## II. QUENCH OF AN INTEGRABLE MODEL AND DYNAMICAL PHASE TRANSITION

### A. Dynamical free energy

For all ramped quench schemes, to be analyzed in the subsequent discussions, we follow the terminology implemented in Refs. [106, 107]. Let us consider an integrable model reducible to a two level Hamiltonian  $H_k(\lambda)$  for each momentum mode and the system is initially ( $t_i \rightarrow -\infty$ ) in the ground state  $|1_k^i\rangle$  of the initial Hamiltonian  $H_k(\lambda_i)$  for each mode. In the ramped quench protocol, the Hamiltonian is characterized by a parameter  $\lambda$  which is quenched from an initial value  $\lambda_i$  at  $t_i$  following the quenching protocol  $\lambda(t) = vt$  to a final value  $\lambda_f$  at  $t_f$ , in such a way that the system crosses the QCP at  $\lambda = \lambda_c$ . Since the condition for an adiabatic dynamics breaks in the vicinity of the QCP, one arrives at a final state  $|\psi_k^f\rangle$  (for the  $k$ -th mode) which may not be the ground state of the final Hamiltonian  $H_k(\lambda_f) = H_k^f$ . The final state can be written in the form of  $|\psi_k^f\rangle = v_k|1_k^f\rangle + u_k|2_k^f\rangle$ , ( $|u_k|^2 + |v_k|^2 = 1$ ) where,  $|1_k^f\rangle$  and  $|2_k^f\rangle$  are the ground and the excited states of the final Hamiltonian  $H_k^f$  with the corresponding energy eigenvalues  $\epsilon_{k,1}^f$  and  $\epsilon_{k,2}^f$ , respectively. Clearly  $p_k = |u_k|^2 = |\langle 2_k^f | 1_k^i \rangle|^2$  denotes the non-adiabatic transition probability that the system ends up at the excited state at the end of quench. Therefore, the Loschmidt overlap for the mode  $k$  for  $t > t_f$  is defined by [106, 107]

$$\mathcal{L}_k = \langle \psi_k^f | \exp(-H_k^f t) | \psi_k^f \rangle = |v_k|^2 \exp(-i\epsilon_{k,1}^f t) + |u_k|^2 \exp(-i\epsilon_{k,2}^f t), \quad (1)$$

and the corresponding dynamical free energy [20, 21],  $g_k(t) = -\log \langle \psi_k^f | \exp(-H_k^f t) | \psi_k^f \rangle / N$ , where  $N$  is the size of the system.

Summing over the contributions from all momentum modes and converting summation to the integral in the thermodynamic limit, one gets [106–108]

$$g(t) = \frac{-1}{2\pi} \int_0^\pi \log \left( 1 + 4p_k(p_k - 1) \sin^2 \left( \frac{\epsilon_{k,2}^f - \epsilon_{k,1}^f}{2} t \right) \right) dk,$$

where  $t$  is measured from the instant the final state,  $|\psi_k^f\rangle$ , is reached at the end of the ramped quench (Fig. 1). The

argument of the logarithm is seen to vanish with  $g(t)$  becoming nonanalytic when  $t = t_n^*$  given by

$$t_n^* = \frac{\pi}{(\epsilon_{k^*,2}^f - \epsilon_{k^*,1}^f)} (2n + 1). \quad (2)$$

These are the critical times for the DQPTs, with  $k^*$  the mode that satisfies  $|u_{k^*}|^2 = p_{k^*} = 1/2$ . For the case  $\epsilon_{k,2}^f = -\epsilon_{k,1}^f = \epsilon_k^f$ , Eq. (2) is simplified to

$$t_n^* = \frac{\pi}{\epsilon_{k^*}^f} \left( n + \frac{1}{2} \right). \quad (3)$$

## B. Dynamical Topological Order Parameter

Analogous to order parameters at equilibrium quantum phase transition, a dynamical topological order parameter is introduced to capture DQPTs [94, 109]. The DTOP is quantized and its unit magnitude jumps at the time of DQPTs reveal the topological aspect of DQPT [94, 97, 99]. This DTOP is extracted from the gauge-invariant Pancharatnam geometric phase associated with the Loschmidt amplitude [94, 110]. The dynamical topological order parameter is defined as [94]

$$W_n(t) = \frac{1}{2\pi} \int_0^\pi \frac{\partial \phi^G(k, t)}{\partial k} dk, \quad (4)$$

where the geometric phase  $\phi^G(k, t)$  is gained from the total phase  $\phi(k, t)$  by subtracting the dynamical phase  $\phi^D(k, t)$ :  $\phi^G(k, t) = \phi(k, t) - \phi^D(k, t)$ . The total phase  $\phi(k, t)$  is the phase factor of Loschmidt amplitude in its polar coordinate representation, i.e.,  $\mathcal{L}_k(t) = |\mathcal{L}_k(t)| e^{i\phi(k, t)}$ , and  $\phi^D(k, t) = -\int_0^t \langle \psi_k^f(t') | H(k, t') | \psi_k^f(t') \rangle dt'$ , in which  $\phi(k, t)$  and  $\phi^D(k, t)$ , for the two level system can be calculated as follows [106, 107]

$$\phi(k, t) = \tan^{-1} \left( \frac{-|u_k|^2 \sin(2\epsilon_k^f t)}{|v_k|^2 + |u_k|^2 \cos(2\epsilon_k^f t)} \right), \quad \phi^D(k, t) = -2|u_k|^2 \epsilon_k^f t,$$

so that [106, 107]

$$\phi_k^G = \tan^{-1} \left( \frac{-|u_k|^2 \sin(2\epsilon_k^f t)}{|v_k|^2 + |u_k|^2 \cos(2\epsilon_k^f t)} \right) + 2|u_k|^2 \epsilon_k^f t. \quad (5)$$

In the following we will study the scaling and universality of DQPTs and the corresponding topological properties (DTOP) of the periodically time dependent extended XY model with linear time dependent transverse field.

## III. MODEL AND EXACT SOLUTION

The Hamiltonian of Floquet spin system in the presence of linear time dependent magnetic field is given as

$$\mathcal{H}(t) = \sum_n \left[ (J + \gamma \cos \omega t) s_n^x s_{n+1}^x + (J - \gamma \cos \omega t) s_n^y s_{n+1}^y - \gamma \sin \omega t (s_n^x s_{n+1}^y + s_n^y s_{n+1}^x) + h(t) s_n^z \right], \quad (6)$$

where  $s_n^\alpha = \sigma_n^\alpha / 2$  ( $\alpha = x, y, z$ ) and  $\sigma_n^\alpha$  are the Pauli matrices, and the transverse magnetic field  $h(t) = h_f + vt$  changes from the initial value  $h_i$  at time  $t = t_i < 0$  to the final values  $h_f$  at  $t = t_f = 0$  with sweep velocity  $v$ .

Performing the Jordan-Wigner fermionization and thanks to the Fourier transformation [111] the Hamiltonian of Eq. (1) can be written as the sum of  $N/2$  non-interacting terms

$$H(t) = \sum_k \mathcal{H}_k(t). \quad (7)$$

with

$$\mathcal{H}_k(t) = [J \cos(k) + h(t)] (c_k^\dagger c_k + c_{-k}^\dagger c_{-k}) + i\gamma \sin(k) (e^{i\omega t} c_k^\dagger c_{-k}^\dagger + e^{-i\omega t} c_k c_{-k}), \quad (8)$$

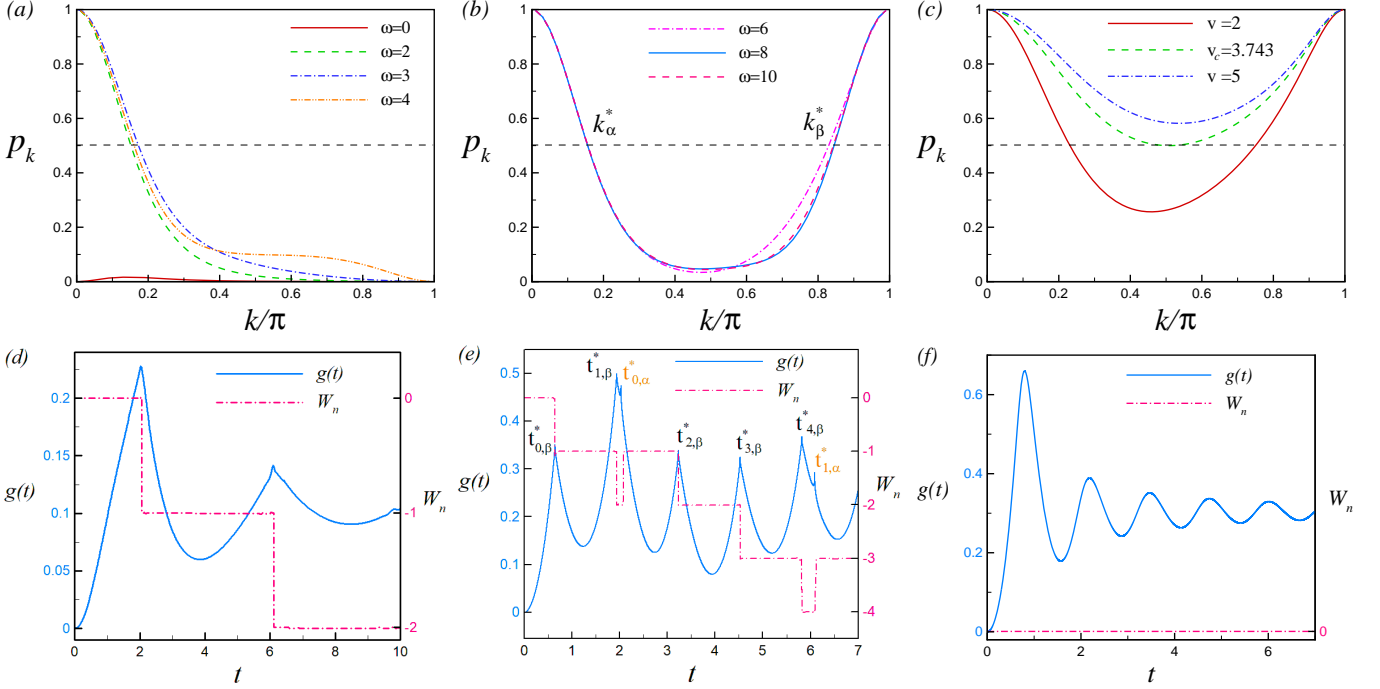


FIG. 2. (Color online) Probabilities  $p_k$  for finding the system with momentum  $k$  in the upper level for sweep velocity  $v = 1$ , (a) for driven frequency  $\omega = 0$  at which the ramp quench does not cross the critical point and also for the ramp across the single critical point  $h_c = -1 - \omega/2$  for  $\omega = 2, 3, 4$ , (b) for the ramp quench that crosses the two critical points  $h_c = -1 - \omega/2$  and  $h_c = 1 - \omega/2$  for  $\omega = 6, 8, 10$ . (c) The excitation probability versus the momentum for a quench across two critical points  $h_c = -4$  and  $h_c = -2$  ( $\omega = 6$ ) for different values of the sweep velocity. The dynamical free energy  $g(t)$  and associated dynamical topological order parameter  $W_n(t)$  (d) for a quench across the single critical point  $h_c = -2$  ( $\omega = 2$ ) for  $v = 1$ , (e) for a quench across two single critical points  $h_c = -5$  and  $h_c = -3$  ( $\omega = 8$ ) for  $v = 1$ , and (f) for a quench across two critical points  $h_c = -4$  and  $h_c = -2$  ( $\omega = 6$ ) for  $v = 5 > v_c = 3.743$ .

where the wave number  $k$  is equal to  $k = (2m - 1)\pi/N$  and  $m$  runs from 1 to  $N/2$ , being  $N$  the total number of spins (sites) in the chain. Eq. (8) implies that the Hamiltonian of  $N$  interacting spins (Eq. (6)) can be mapped to the sum of  $N/2$  noninteracting quasi-spins.

The Bloch single particle Hamiltonian  $\mathcal{H}_k(t)$  can be written as

$$\mathcal{H}_k(t) = \begin{pmatrix} h_z(k, t) & ih_{xy}(k)e^{i\omega t} \\ -ih_{xy}(k)e^{-i\omega t} & -h_z(k, t) \end{pmatrix}, \quad (9)$$

with  $h_{xy}(k) = \gamma \sin(k)$ , and  $h_z(k, t) = J \cos(k) + h(t)$ , which is exactly the same as twisted Landau-Zener Hamiltonian [112–115]. Due to the explicit time dependence in Hamiltonian Eq.(6), the instantaneous eigenvalues and eigenvectors are given by

$$\varepsilon_k^\pm = \pm \varepsilon_k = \pm \sqrt{h_z^2(k, t) + h_{xy}^2(k)}, \quad (10)$$

$$|\chi_k^-(t)\rangle = e^{i\omega t} \cos\left(\frac{\theta_k}{2}(t)\right) |\uparrow\rangle - i \sin\left(\frac{\theta_k}{2}(t)\right) |\downarrow\rangle, \quad |\chi_k^+(t)\rangle = -i \sin\left(\frac{\theta_k}{2}(t)\right) |\uparrow\rangle + e^{-i\omega t} \cos\left(\frac{\theta_k}{2}(t)\right) |\downarrow\rangle,$$

where,

$$\cos\left(\frac{\theta_k}{2}\right) = \frac{(\varepsilon_k - h_z(k, t))}{\sqrt{2\varepsilon_k(\varepsilon_k - h_z(k, t))}}, \quad \sin\left(\frac{\theta_k}{2}\right) = \frac{h_{xy}}{\sqrt{2\varepsilon_k(\varepsilon_k - h_z(k, t))}},$$

and  $|\chi_{k,t}^\pm\rangle$  are the adiabatic basis of the system.

If the system is prepared in its ground state at  $t_i \rightarrow -\infty$  ( $h_i \ll h_c = -1$ ), ( $a_1(t_i) = 1$ ,  $a_2(t_i) = 0$ ) as explained in Appendix B) the probability that the  $k$ :th mode is found in the upper level at  $t$  is given as

$$p_k = |U_{22} \cos(\vartheta_k(t)/2) + U_{12} \sin(\vartheta_k(t)/2)|^2, \quad (11)$$

with,

$$U_{12}(z) = \frac{\Gamma(1-\nu)}{\alpha\sqrt{\pi}} e^{i\pi/4} [D_\nu(z_i)D_\nu(-z) - D_\nu(-z_i)D_\nu(z)], \quad U_{22}(z) = \frac{\Gamma(1-\nu)}{\sqrt{2\pi}} [D_\nu(-z_i)D_{\nu-1}(z) + D_\nu(z_i)D_{\nu-1}(-z)],$$

where,  $D_\nu(z)$  is the parabolic cylinder function [116, 117],  $\Gamma(x)$  is the Euler gamma function [116, 117]  $\alpha = \gamma \sin(k)/\sqrt{v}$ ,  $\nu = i\alpha^2/2$ ,  $z = e^{-i\pi/4}\sqrt{2v}\tau_k$ ,  $z_i = e^{-i\pi/4}\sqrt{2v}\tau_{k,i}$ ,  $\tau_{k,i} = (h_f + vt_i + J \cos(k) + \omega/2)/v$ , and

$$\cos\left(\frac{\vartheta_k(t)}{2}\right) = \frac{\tilde{\varepsilon}_k - (h_z(k, t) + \omega/2)}{\sqrt{2\tilde{\varepsilon}_k[\tilde{\varepsilon}_k - (h_z(k, t) + \omega/2)]}}, \quad \sin\left(\frac{\vartheta_k(t)}{2}\right) = \frac{h_{xy}}{\sqrt{2\tilde{\varepsilon}_k[\tilde{\varepsilon}_k - (h_z(k, t) + \omega/2)]}}. \quad (12)$$

with  $\tilde{\varepsilon}_k = \sqrt{(h_z(k, t) + \omega/2)^2 + h_{xy}^2(k)}$ . It should be mentioned that, when the magnetic field is time-independent  $h(t) = h$ , the Floquet Hamiltonian in the rotating frame given by the unitary transformation  $U_R(t) = \exp[i\omega(\sigma^z)t/2]$  [16, 87, 89, 91–93], is transformed to the time-independent Hamiltonian

$$\mathbb{H}_k = [h_{xy}(k)\sigma^x + (h_z(k) + \omega/2)\sigma^z]. \quad (13)$$

It can be verified that the effective time-independent Hamiltonian undergoes quantum phase transitions at  $h_c = \pm J - \omega/2$ , where the energy gap closes at  $k = 0, \pi$  [16, 93]. Therefore the critical points of the effective Hamiltonian can be displaced by tuning the driven frequency.

## IV. NUMERICAL RESULTS

In this section, we report the results of our numerical simulations, based on an analytical approach, to investigate the dynamics of model using the notion of the DQPTs. To this end, we consider the linear quenching of the transverse field  $h(t) = h_f + vt$ , changes from initial value  $h_i = -20$  at  $t_i = (h_i - h_f)/v$ , where the system is prepared in its ground state, to the final values  $h_f = -1.5$  at  $t_f = 0$ . If we set  $J$  to unity, the critical points of the model are given as  $h_c = -1 - \omega/2$  ( $k = 0$ ) and  $h_c = 1 - \omega/2$  ( $k = \pi$ ).

### A. Dynamical free energy and DTOP

#### 1. Quench across a single critical point

For the ramp quench crosses the single critical point  $h_c = -1 - \omega/2$  at  $k = 0$ , the excitation probability after the ramp quench depends on the value of  $k$ . It is obvious that the modes close to gap closing mode  $k = 0$  are frozen in the process of quenching as the off-diagonal terms in Hamiltonian Eq. (13) vanish and hence  $p_{k=0} = 1$ . While away from the gap closing mode the system evolves adiabatically and can be shown  $p_{k \rightarrow \pi} \rightarrow 0$ . Given these two limiting cases, continuity of the transition probability as a function of  $k$  in the thermodynamic limit, implies that there exists a critical mode  $k^*$  at which  $p_{k^*} = 1/2$  and consequently DQPTs appear. The transition probability has been plotted versus  $k$  in Fig. 2(a) for sweep velocity  $v = 1$ , and for driven frequency  $\omega = 0$  which  $h_c = -1$  and also for the ramp across the single critical point  $h_c = -1 - \omega/2$  for  $\omega = 2, 3, 4$ . Since the ramp quench does not cross the critical point for  $\omega = 0$ , the excitation probability is very small. However,  $p_{k=0} = 1$  for the driven frequencies  $\omega = 2, 3, 4$  at which the quench crosses the single critical point and the transition probability is negligible away from the gap closing mode ( $k \rightarrow \pi$ ). From these observations, it is straightforward to conclude that there is always a critical momentum  $k^*$  and hence those of  $t_n^*$ , related through Eq. (3), which get modified when  $v$  is changed. In other words, different values of sweep velocity simply results in a different sequence of DQPTs time. The existence of DQPTs for  $v \rightarrow \infty$  is expected, since  $k^*$  is always present for a sudden quench across a single QCP, as reported in Ref. [20].

#### 2. Quench across two critical points

Performing a quench across both equilibrium critical points  $h_c = \pm 1 - \omega/2$  shows new features. Here the field is swept from one equilibrium paramagnetic ground state to another one, and if the quench is sudden it is not expected

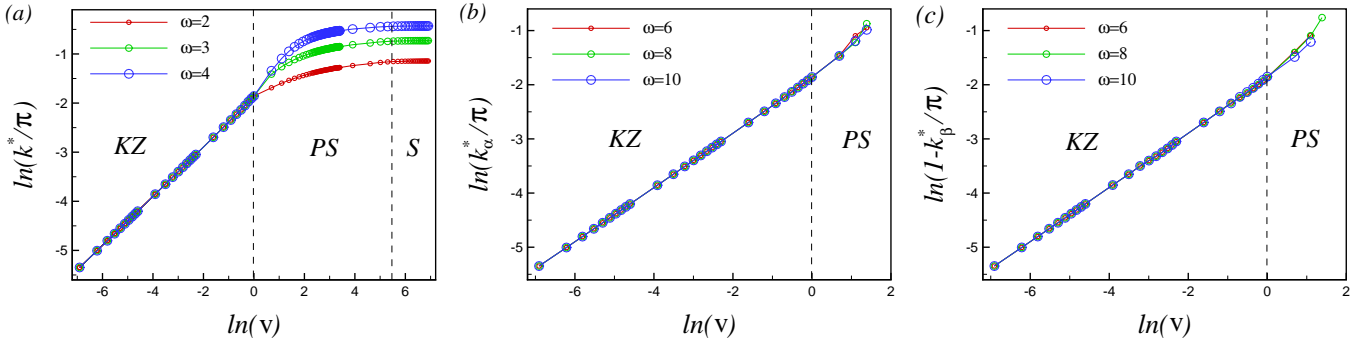


FIG. 3. (Color online) Scaling of the critical mode versus sweep velocity for (a) quench crossing a single critical mode  $h_c = -1 - \omega/2$  ( $\omega = 2, 3, 4$ ), (b) and (c) quench across two critical points  $h_c = -1 - \omega/2$  and  $h_c = 1 - \omega/2$  ( $\omega = 6, 8, 10$ ). For a quench that crosses two critical points, there exist a critical velocity above which DQPT is wiped out. Therefore, the scaling behavior of the critical modes include just Kibble-Zurek and pre-saturated regions.

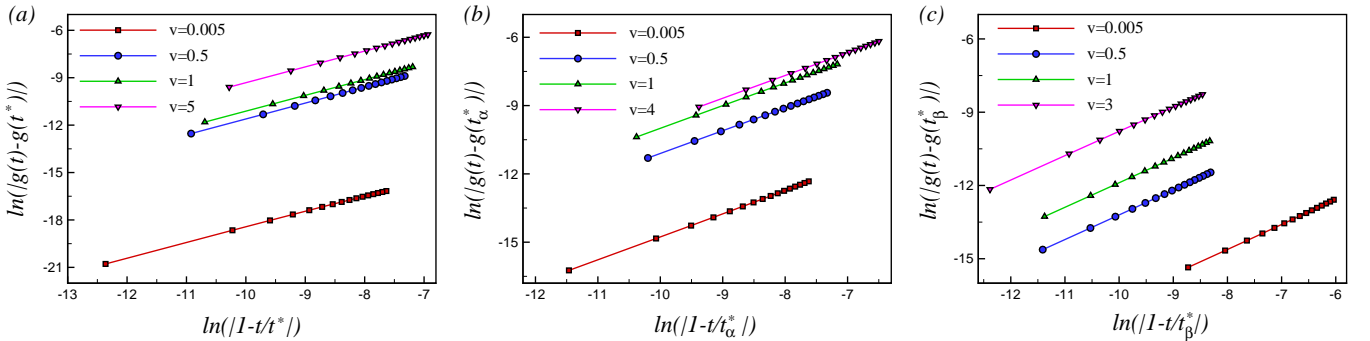


FIG. 4. (Color online) . Scaling analysis of the dynamical free energy close to the critical time for both cases of the ramp quench for different values of the sweep velocity (a)  $\omega = 2$ , (b)  $\omega = 6$  and close to  $t_\alpha^*$  and (c)  $\omega = 6$  and close to  $t_\beta^*$ .

to result in DQPTs [44, 107, 108]. For a quench crossing both critical points, the off-diagonal terms in the Hamiltonian Eq. (13) are temporally frozen and consequently leading to  $p_{k=0} = p_{k=\pi} = 1$ . As discussed, the maximum value of transition probability  $p_{k=0,\pi} = 1$  is greater than  $1/2$ , the occurrence of DQPTs requires the condition that the minimum value of the non-adiabatic transition probability must be less than  $1/2$ . Thus, making the quench sufficiently slow ( $v < v_c$ ) ensures that the excitation probability for modes away from the gap closing ones is smaller than  $1/2$  and sets of a succession of DQPTs. In Fig. 2(b) the transition probability has been shown versus  $k$  for driven frequencies  $\omega = 6, 8, 10$  for  $v = 1$ . As predicted,  $p_{k=0,\pi} = 1$  and the minimum of  $p_k$  away from the critical modes is less than  $1/2$  for the small sweep velocity. In such a case, there is two critical modes  $k_\alpha^*$  and  $k_\beta^*$  at which  $p_{k_\alpha^*,\beta} = 1/2$  yields a sequence of DQPTs at the corresponding critical times  $t_n^* = t_{n,\alpha}^*, t_{n,\beta}^*, n = 0, 1, \dots$

The probability of excitation has been plotted versus  $k$  for  $\omega = 6$  for different values of sweep velocity in Fig. 2(c). As seen there is a threshold sweep velocity  $v_c = 3.743$  above which the minimum of  $p_k$  is greater than  $1/2$  and DQPTs get completely wiped out.

The dynamical free energy and DTOP of the model have been depicted in Figs. 2(d)-(f) for two cases of the ramped quench. Fig. 2(d) represents the dynamical free energy and DTOP for a quench crossing a single critical point  $h_c = -2$  ( $\omega = 2$ ). Cusps in  $g(t)$  and quantizations in the associated DTOP ( $W_n(t)$ ) are clearly visible as an indicator of DQPTs.

The dynamical free energy and DTOP for a quench across two critical points  $h_c = -5$  and  $h_c = -3$ , ( $\omega = 8$ ) have been depicted in Fig. 2(e). The DQPTs show up as cusps in the dynamical free energy  $g(t)$  and, more visibly, as steps in the associated DTOP ( $W_n(t)$ ).

Fig. 2(f) displays dynamical free energy and DTOP for a quench that ramp crossing two critical points for  $\omega = 6$  for sweep velocity  $v = 5$ . As seen, above the critical sweep velocity  $v = 5 > v_c = 3.743$ , a maximally mixed state  $p_k = 1/2$  does not appear at the end of the quench, thus blocking the appearance of DQPTs.



## B. Scaling of the critical modes

Here, we give a comprehensive characterization of the dynamical properties of the ramped quench DQPTs. To this end, we make the distinction between critical modes of very slow, fast, and very fast ramped quench DQPTs by determining the crossover points between the three different regions. As a main result, we obtain the behaviour of critical modes as a function of sweep velocity for each region.

**KZ Region:** In KZ region the sweep velocity is very small so that we can consider  $\tau_{k,t_i} \rightarrow -\infty$ . On the other hand,  $\tau_{k,t_f} = (h_f + J \cos(k) + \omega/2)/v \gg \tau_T = \gamma \sin(k)/v$ , for  $k \ll \pi/4$ , where  $\tau_T$  is the tunneling time in the adiabatic limit of Landau-Zener model [118]. Therefore, the final time instance is well outside the transition time interval for long wavelength modes and  $\tau_{k,t_f}$  can be extended to  $+\infty$  [119]. In other words, only long wavelength modes can get excited in slow quench. In such a case, we can use Landau-Zener equation for excitation probability  $p_k = \exp[-\pi(\gamma \sin(k))^2/v]$  which reduces to  $p_k = \exp(-\pi\gamma^2 k^2/v)$  for long wavelength modes. The critical mode at which the DQPTs happen is given as  $k^* = \sqrt{v \ln(2)/\pi\gamma^2}$ . Thus the critical mode scales linearly with the square root of the sweep velocity  $v$  in KZ region. It has also been shown that, in this region the average density of defects excited scales like a square root of the transition rate [119]. The dependence of the critical mode on the sweep velocity has been shown in Fig. 2(a)-(c) for two cases of the ramped quench, crossing the single critical point (Fig. 3(a)) and crossing two critical points (Fig. 3(b)-(c)), for different values of the driven frequency. The numerical results show that the critical mode in KZ region collapses on a single curve for all driven frequencies which means that the scaling behaviour of the critical mode is independent of the distance between the final quench field end and the critical point. The numerical analysis confirms that, critical mode scales linearly with the sweep velocity with the exponent  $\nu = 1/2 \pm 0.01$ .

**PS Region:** In this region although the quench is fast  $v > 1$  but not so fast to have  $\tau_{k,t_i} \ll 1$ . One can ensure this situation by preparing the initial system far from the critical point  $|h_i| \gg |h_c|$  and also  $|h_i + \omega/2|/\sqrt{v} > 1$ . Moreover,  $\tau_{k,t_f}$  falls into the tunneling interval time so that we can consider  $\tau_{k,t_f} \rightarrow 0$ . As seen in Fig. 3(a)-(c), the critical mode curves belong to the different driven frequency start to get split as the sweep velocity gets faster than one ( $v > 1$ ), for both cases of the ramped quench and enhances non-linearly with the sweep velocity. For a quench across the single critical point (Fig. 3(a)) the critical mode enhances with sweep velocity till  $v \approx |h_i + \omega/2|^2$ . While in the case of quench that crosses two critical points the PS region is confined between the sweep velocity  $v \approx 1$ , below which the system is in KZ region, and the critical sweep velocity  $v_c$ , above which the DQPT is disappeared (Fig. 3(b)-(c)).

**S Region:** In the saturated region, which appears just in a quench across the single critical point (Fig. 3(a)) the quench is so fast that the evolution lasts only for a short period of time. Hence both initial and final times are well inside the tunneling time interval and both  $\tau_{k,t_i}$  and  $\tau_{k,t_f}$  are small such that we can consider  $\tau_{k,t_i}, \tau_{k,t_f} \rightarrow 0$ , which requires  $|h_{i,f} + \omega/2|/\sqrt{v} \ll 1$ . In this region the critical mode makes a plateau versus the sweep velocity. This region shrinks with  $|h_i|$  enhancing until it vanishes in the limit  $|h_i + \omega/2| \rightarrow \infty$  so that the PS regime prevails the entire fast quench regime.

## C. Scaling of dynamical free energy

As mentioned, DQPTs at critical times appear as nonanalyticities during nonequilibrium real-time quantum evolution. In a spirit similar to the equilibrium phase transitions, a major challenge in this work is to seek the fundamental concepts such as scaling and universality in the ramped quench DQPTs. It has been proved that the dynamical free energy shows scaling close to the critical time [120] at a sudden quench. In a one dimensional system the dynamical free energy shows power law scaling close to the DQPT time

$$|g(t) - g(t^*)| \sim \left| \frac{t - t^*}{t^*} \right|^\nu,$$

with an exponent  $\nu = 1$ , while the scaling law in two dimensional systems is logarithmic [120]. On this basis, we have numerically probed the scaling of the dynamical free energy for two cases of the ramped quench for different values of sweep velocity and driven frequency. The scaling behaviour of dynamical free energy close to the critical time  $t^*$  has been plotted in Fig. 4(a) for a quench across the single critical point  $h_c = -1$  ( $\omega = 2$ ), and for a quench that crosses two critical points  $h_c = -4$  and  $h_c = -2$  ( $\omega = 6$ ) in Fig. 4(b)-(c) for different values of sweep velocity. Our numerical simulation reveals that the dynamical free energy shows power law scaling close to the critical time with the exponent  $\nu = 1 \pm 0.01$  which shows the same behavior as given in the sudden quench.

## V. SUMMARY AND DISCUSSION

In this paper, we have studied the non-equilibrium dynamics of the periodically driven extended XY model in the presence of the linear time dependent magnetic field. We show that the critical points of the model can be controlled by the driven frequency. We take advantage of this property to examine the nonequilibrium dynamics of the model after a ramped quench of the magnetic field. For a quench across one of the equilibrium quantum critical points, we find that the critical mode at which DQPTs happens, can be classified into three regions, Kibble-Zurek, pre-saturated and saturated regions. In the Kibble-Zurek region, where the sweep velocity is very small ( $v < 1$ ), the critical mode scales linearly with the square root of the sweep velocity. In this region all curves of the critical mode for different values of the driven frequency collapse on a single curve which indicates that the scaling properties is independent of the distance between the equilibrium phase transition point and the final magnetic field. In the pre-saturated region where sweep velocity redirected between  $v > 1$  and square of the initial magnetic field ( $v < |h_i + \omega/2|^2$ ), the curves of the critical mode for different values of the driven frequency are splitted and the critical mode does not show any specific scaling. In the saturated region  $v > |h_i + \omega/2|^2$ , although curves of the critical mode for different driven frequency are splitted but all curves make a plateau versus the sweep velocity. The saturated region shrinks by increasing the initial magnetic field and disappear in the limit  $|h_i + \omega/2| \rightarrow \infty$  so that the PS region dominates the entire fast quench region. For a quench that crosses two critical points, there exist a critical velocity above which DQPT is wiped out. In the latter case, the scaling behavior of the critical modes include just Kibble-Zurek and pre-saturated regions. In addition, our numerical simulations have shown that the dynamical free energy close to the DQPTs time shows power law scaling with the exponent  $\nu = 1 \pm 0.01$  for all sweep velocities and driven frequencies, which behaves the same as the sudden quench scaling features of the one dimensional systems.

### Appendix A: Jordan-Wigner transformation

The Jordan-Wigner fermionization is defined by following relations

$$s_n^+ = s_n^x + i s_n^y = \prod_{m=1}^{n-1} (1 - 2c_m^\dagger c_m) c_n^\dagger, \quad s_n^- = s_n^x - i s_n^y = \prod_{m=1}^{n-1} c_n (1 - 2c_m^\dagger c_m), \quad s_n^z = s_n^+ s_n^- - \frac{1}{2} = 2c_n^\dagger c_n - 1.$$

where  $c_n^\dagger, c_n$  are the spinless fermion creation and annihilation operators, respectively, and applying the Fourier transform

$$c_n = \frac{1}{\sqrt{N}} \sum_k c_k e^{-ikn}, \quad c_n^\dagger = \frac{1}{\sqrt{N}} \sum_k c_k^\dagger e^{ikn},$$

the Hamiltonian of Eq. (6) can be written as the sum of  $N/2$  non-interacting terms

$$H(t) = \sum_k \mathcal{H}_k(t). \quad (\text{A1})$$

### Appendix B: Time-dependent Schrödinger equation in the diabatic basis

The time-dependent Schrödinger equation of Hamiltonian in Eq. (7) is given as

$$i \frac{d}{dt} \begin{pmatrix} a_1(t) \\ a_2(t) \end{pmatrix} = \mathcal{H}_k(t) \begin{pmatrix} a_1(t) \\ a_2(t) \end{pmatrix}. \quad (\text{B1})$$

To solve the time-dependent Schrödinger equation, we first use the transformation

$$\begin{pmatrix} a_1(t) \\ a_2(t) \end{pmatrix} = S \begin{pmatrix} \tilde{a}_1(t) \\ \tilde{a}_2(t) \end{pmatrix}, \quad (\text{B2})$$

with

$$S = \begin{pmatrix} 0 & i e^{i\omega t/2} e^{-i\pi/4} \\ -i e^{-i\omega t/2} e^{i\pi/4} & 0 \end{pmatrix}, \quad (\text{B3})$$



which results in

$$i \frac{d}{dt} \begin{pmatrix} \tilde{a}_2(t) \\ \tilde{a}_1(t) \end{pmatrix} = \begin{pmatrix} -(h_z(k, t) + \frac{\omega}{2}) & \gamma \sin(k) \\ \gamma \sin(k) & h_z(k, t) + \frac{\omega}{2} \end{pmatrix} \begin{pmatrix} \tilde{a}_2(t) \\ \tilde{a}_1(t) \end{pmatrix}. \quad (\text{B4})$$

The time-dependent Schrödinger equation (9) is mapped to the time-dependent Schrödinger equation of Landau-Zener problem [121, 122] by defining the new time scale  $\tau_k = (h_f + vt + J \cos(k) + \omega/2)/v$ ,

$$i \frac{d}{d\tau_k} \begin{pmatrix} \tilde{a}_2(\tau_k) \\ \tilde{a}_1(\tau_k) \end{pmatrix} = \begin{pmatrix} -v\tau_k & \gamma \sin(k) \\ \gamma \sin(k) & v\tau_k \end{pmatrix} \begin{pmatrix} \tilde{a}_2(\tau_k) \\ \tilde{a}_1(\tau_k) \end{pmatrix}. \quad (\text{B5})$$

The Landau-Zener problem is exactly solvable as explained in Refs. [121, 122]

$$\begin{pmatrix} \tilde{a}_2(\tau_k) \\ \tilde{a}_1(\tau_k) \end{pmatrix} = \begin{pmatrix} U_{11} & U_{12} \\ U_{21} & U_{22} \end{pmatrix} \begin{pmatrix} \tilde{a}_2(\tau_{k,i}) \\ \tilde{a}_1(\tau_{k,i}) \end{pmatrix}, \quad (\text{B6})$$

where,

$$\begin{aligned} U_{11}(z) &= \frac{\Gamma(1-\nu)}{\sqrt{2\pi}} \left[ D_{\nu-1}(-z_i) D_\nu(z) + D_{\nu-1}(z_i) D_\nu(-z) \right], & U_{12}(z) &= \frac{\Gamma(1-\nu)}{\alpha \sqrt{\pi}} e^{i\pi/4} \left[ D_\nu(z_i) D_\nu(-z) - D_\nu(-z_i) D_\nu(z) \right], \\ U_{21}(z) &= \frac{\alpha \Gamma(1-\nu)}{2\sqrt{\pi}} e^{-i\pi/4} \left[ D_{\nu-1}(z_i) D_{\nu-1}(-z) - D_{\nu-1}(-z_i) D_{\nu-1}(z) \right], \\ U_{22}(z) &= \frac{\Gamma(1-\nu)}{\sqrt{2\pi}} \left[ D_\nu(-z_i) D_{\nu-1}(z) + D_\nu(z_i) D_{\nu-1}(-z) \right], \end{aligned} \quad (\text{B7})$$

where,  $D_\nu(z)$  is the parabolic cylinder function [116, 117],  $\alpha = \gamma \sin(k)/\sqrt{v}$ ,  $\nu = i\alpha^2/2$ ,  $z = e^{-i\pi/4} \sqrt{2v} \tau_k$ ,  $z_i = e^{-i\pi/4} \sqrt{2v} \tau_{k,i}$  and  $\tau_{k,i} = (h_f + vt_i + J \cos(k) + \omega/2)/v$ .

Using the transformation given in Eq. (B2), we can transform  $\tilde{a}_m(\tau_k)$  to  $a_m(t)$  ( $m = 1, 2$ )

$$\begin{aligned} S(t) \begin{pmatrix} \tilde{a}_2(\tau_k) \\ \tilde{a}_1(\tau_k) \end{pmatrix} &= S(t) \begin{pmatrix} U_{11} & U_{12} \\ U_{21} & U_{22} \end{pmatrix} S^\dagger(t_i) S(t_i) \begin{pmatrix} \tilde{a}_2(\tau_{k,i}) \\ \tilde{a}_1(\tau_{k,i}) \end{pmatrix}, \\ \begin{pmatrix} a_1(t) \\ a_2(t) \end{pmatrix} &= S(t) \begin{pmatrix} U_{11} & U_{12} \\ U_{21} & U_{22} \end{pmatrix} S^\dagger(t_i) \begin{pmatrix} a_1(t_i) \\ a_2(t_i) \end{pmatrix}. \end{aligned}$$

### Appendix C: Exact solution in the adiabatic basis

The adiabatic solution can be obtained by transforming Eqs. (B1) into the adiabatic representation by the unitary transformation

$$R = \begin{pmatrix} e^{i\omega t/2} \sin(\vartheta_k(t)/2) & i e^{i\omega t/2} \cos(\vartheta_k(t)/2) \\ i e^{-i\omega t/2} \cos(\vartheta_k(t)/2) & e^{-i\omega t/2} \sin(\vartheta_k(t)/2) \end{pmatrix} \quad (\text{C1})$$

where,

$$\cos\left(\frac{\vartheta_k(t)}{2}\right) = \frac{\tilde{\varepsilon}_k - (h_z(k, t) + \omega/2)}{\sqrt{2\tilde{\varepsilon}_k[\tilde{\varepsilon}_k - (h_z(k, t) + \omega/2)]}}, \quad \sin\left(\frac{\vartheta_k(t)}{2}\right) = \frac{h_{xy}}{\sqrt{2\tilde{\varepsilon}_k[\tilde{\varepsilon}_k - (h_z(k, t) + \omega/2)]}},$$

with  $\tilde{\varepsilon}_k = \sqrt{(h_z(k, t) + \omega/2)^2 + h_{xy}^2(k)}$ .

$$\begin{pmatrix} a_1^A(t) \\ a_2^A(t) \end{pmatrix} = R^\dagger \begin{pmatrix} a_1(t) \\ a_2(t) \end{pmatrix}. \quad (\text{C2})$$

In the limit  $\tau_k \gg \gamma \sin(k)$ , the adiabatic eigenstates coincide with the diabatic states. If the system is prepared in its ground state at  $t_i \rightarrow -\infty$  ( $h_i \ll h_c = -1$ ), i.e.,  $a_1(t_i) = 1$ ,  $a_2(t_i) = 0$  the probability that the  $k$ :th mode is found in the upper level at  $t$  is given as  $p_k = |U_{22} \cos(\vartheta_k(t)/2) + U_{12} \sin(\vartheta_k(t)/2)|^2$ .

---

[1] A. Polkovnikov, K. Sengupta, A. Silva, and M. Vengalattore, Colloquium: Nonequilibrium dynamics of closed interacting quantum systems, *Rev. Mod. Phys.* **83**, 863 (2011).

- [2] M. A. Cazalilla, R. Citro, T. Giamarchi, E. Orignac, and M. Rigol, One dimensional bosons: From condensed matter systems to ultracold gases, *Rev. Mod. Phys.* **83**, 1405 (2011).
- [3] D. Bernard and B. Doyon, Conformal field theory out of equilibrium: a review, *Journal of Statistical Mechanics: Theory and Experiment* **2016**, 064005 (2016).
- [4] C. Gogolin and J. Eisert, Equilibration, thermalisation, and the emergence of statistical mechanics in closed quantum systems, *Reports on Progress in Physics* **79**, 056001 (2016).
- [5] D. A. Abanin, E. Altman, I. Bloch, and M. Serbyn, Colloquium: Many-body localization, thermalization, and entanglement, *Rev. Mod. Phys.* **91**, 021001 (2019).
- [6] A. Nava, C. A. Perroni, R. Egger, L. Lepori, and D. Giuliano, Lindblad master equation approach to the dissipative quench dynamics of planar superconductors, arXiv preprint arXiv:2308.08264 (2023).
- [7] A. Nava, C. A. Perroni, R. Egger, L. Lepori, and D. Giuliano, Dissipation driven dynamical topological phase transitions in two-dimensional superconductors, arXiv preprint arXiv:2308.08265 (2023).
- [8] G. Jotzu, M. Messer, R. Desbuquois, M. Lebrat, T. Uehlinger, D. Greif, and T. Esslinger, Experimental realization of the topological haldane model with ultracold fermions, *Nature* **515**, 237 (2014).
- [9] A. J. Daley, H. Pichler, J. Schachenmayer, and P. Zoller, Measuring entanglement growth in quench dynamics of bosons in an optical lattice, *Phys. Rev. Lett.* **109**, 020505 (2012).
- [10] M. Schreiber, S. S. Hodgman, P. Bordia, H. P. Lüschen, M. H. Fischer, R. Vosk, E. Altman, U. Schneider, and I. Bloch, Observation of many-body localization of interacting fermions in a quasirandom optical lattice, *Science* **349**, 842 (2015).
- [11] N. Fläschner, D. Vogel, M. Tarnowski, B. S. Rem, D.-S. Lühmann, M. Heyl, J. C. Budich, L. Mathey, K. Sengstock, and C. Weitenberg, Observation of dynamical vortices after quenches in a system with topology, *Nature Physics* **14**, 265 (2017).
- [12] I. Bloch, J. Dalibard, and W. Zwerger, Many-body physics with ultracold gases, *Rev. Mod. Phys.* **80**, 885 (2008).
- [13] P. Jurcevic, H. Shen, P. Hauke, C. Maier, T. Brydges, C. Hempel, B. P. Lanyon, M. Heyl and, R. Blatt, and C. F. Roos, Direct observation of dynamical quantum phase transitions in an interacting many-body system, *Phys. Rev. Lett.* **119**, 080501 (2017).
- [14] E. A. Martinez, C. A. Muschik, P. Schindler, D. Nigg, A. Erhard, M. Heyl, P. Hauke, M. Dalmonte, T. Monz, P. Zoller, *et al.*, Real-time dynamics of lattice gauge theories with a few-qubit quantum computer, *Nature* **534**, 516 (2016).
- [15] J. Smith, A. Lee, P. Richerme, B. Neyenhuis, P. W. Hess, P. Hauke, M. Heyl, D. A. Huse, and C. Monroe, Many-body localization in a quantum simulator with programmable random disorder, *Nature Physics* **12**, 907 (2016).
- [16] K. Yang, L. Zhou, W. Ma, X. Kong, P. Wang, X. Qin, X. Rong, Y. Wang, F. Shi, J. Gong, and J. Du, Floquet dynamical quantum phase transitions, *Phys. Rev. B* **100**, 085308 (2019).
- [17] X.-Y. Guo, C. Yang, Y. Zeng, Y. Peng, H.-K. Li, H. Deng, Y.-R. Jin, S. Chen, D. Zheng, and H. Fan, Observation of a dynamical quantum phase transition by a superconducting qubit simulation, *Phys. Rev. Applied* **11**, 044080 (2019).
- [18] K. Wang, X. Qiu, L. Xiao, X. Zhan, Z. Bian, W. Yi, and P. Xue, Simulating dynamic quantum phase transitions in photonic quantum walks, *Phys. Rev. Lett.* **122**, 020501 (2019).
- [19] X.-Y. Xu, Q.-Q. Wang, M. Heyl, J. C. Budich, W.-W. Pan, Z. Chen, M. Jan, K. Sun, J.-S. Xu, Y.-J. Han, *et al.*, Measuring a dynamical topological order parameter in quantum walks, *Light: Science & Applications* **9**, 1 (2020).
- [20] M. Heyl, A. Polkovnikov, and S. Kehrein, Dynamical quantum phase transitions in the transverse-field ising model, *Phys. Rev. Lett.* **110**, 135704 (2013).
- [21] M. Heyl, Dynamical quantum phase transitions: a review, *Reports on Progress in Physics* **81**, 054001 (2018).
- [22] R. Jafari, H. Johannesson, A. Langari, and M. A. Martin-Delgado, Quench dynamics and zero-energy modes: The case of the creutz model, *Phys. Rev. B* **99**, 054302 (2019).
- [23] K. Najafi, M. A. Rajabpour, and J. Viti, Light-cone velocities after a global quench in a noninteracting model, *Phys. Rev. B* **97**, 205103 (2018).
- [24] R. Jafari and H. Johannesson, Loschmidt echo revivals: Critical and noncritical, *Phys. Rev. Lett.* **118**, 015701 (2017).
- [25] K. Najafi, M. A. Rajabpour, and J. Viti, Return amplitude after a quantum quench in the XY chain, *Journal of Statistical Mechanics: Theory and Experiment* **2019**, 083102 (2019).
- [26] B. Yan, L. Cincio, and W. H. Zurek, Information scrambling and loschmidt echo, *Phys. Rev. Lett.* **124**, 160603 (2020).
- [27] T. V. Zache, N. Mueller, J. T. Schneider, F. Jendrzejewski, J. Berges, and P. Hauke, Dynamical topological transitions in the massive schwinger model with a  $\theta$  term, *Phys. Rev. Lett.* **122**, 050403 (2019).
- [28] S. Mukherjee and T. Nag, Dynamics of decoherence of an entangled pair of qubits locally connected to a one-dimensional disordered spin chain, *Journal of Statistical Mechanics: Theory and Experiment* **2019**, 043108 (2019).
- [29] J. M. Zhang and H.-T. Yang, Sudden jumps and plateaus in the quench dynamics of a bloch state, *EPL (Europhysics Letters)* **116**, 10008 (2016).
- [30] J. M. Zhang and H.-T. Yang, Cusps in the quench dynamics of a bloch state, *EPL (Europhysics Letters)* **114**, 60001 (2016).
- [31] M. Serbyn and D. A. Abanin, Loschmidt echo in many-body localized phases, *Phys. Rev. B* **96**, 014202 (2017).
- [32] M. Sadrzadeh, R. Jafari, and A. Langari, Dynamical topological quantum phase transitions at criticality, *Phys. Rev. B* **103**, 144305 (2021).
- [33] K. Cao, M. Zhong, and P. Tong, Dynamical quantum phase transition in periodic quantum ising chains, *Journal of Physics A: Mathematical and Theoretical* **55**, 365001 (2022).
- [34] C. Y. Wong and W. C. Yu, Loschmidt amplitude spectrum in dynamical quantum phase transitions, *Phys. Rev. B* **105**, 174307 (2022).

- [35] A. Sehrawat, C. Srivastava, and U. Sen, Dynamical phase transitions in the fully connected quantum ising model: Time period and critical time, *Phys. Rev. B* **104**, 085105 (2021).
- [36] C. Rylands, E. A. Yuzbashyan, V. Gurarie, A. Zabalo, and V. Galitski, Loschmidt echo of far-from-equilibrium fermionic superfluids, *Annals of Physics* **435**, 168554 (2021), special issue on Philip W. Anderson.
- [37] M. Kloc, D. Šimsa, F. Hanák, P. R. Kaprálová-Žďánská, P. Stránský, and P. Cejnar, Quasiclassical approach to quantum quench dynamics in the presence of an excited-state quantum phase transition, *Phys. Rev. A* **103**, 032213 (2021).
- [38] S. Bhattacharyya and S. Dasgupta, Exotic signature of dynamical quantum phase transition in the time evolution of an engineered initial state, *Journal of Physics A: Mathematical and Theoretical* **53**, 265002 (2020).
- [39] M. Abdi, Dynamical quantum phase transition in bose-einstein condensates, *Phys. Rev. B* **100**, 184310 (2019).
- [40] J. Knaute, Meson content of entanglement spectra after integrable and nonintegrable quantum quenches, *Phys. Rev. B* **107**, L100303 (2023).
- [41] F. Andraschko and J. Sirker, Dynamical quantum phase transitions and the loschmidt echo: A transfer matrix approach, *Phys. Rev. B* **89**, 125120 (2014).
- [42] S. Vajna and B. Dóra, Topological classification of dynamical phase transitions, *Phys. Rev. B* **91**, 155127 (2015).
- [43] C. Karrasch and D. Schuricht, Dynamical phase transitions after quenches in nonintegrable models, *Phys. Rev. B* **87**, 195104 (2013).
- [44] S. Vajna and B. Dóra, Disentangling dynamical phase transitions from equilibrium phase transitions, *Phys. Rev. B* **89**, 161105 (2014).
- [45] R. Jafari, Dynamical quantum phase transition and quasi particle excitation, *Scientific reports* **9**, 2871 (2019).
- [46] D. Mondal and T. Nag, Anomaly in the dynamical quantum phase transition in a non-hermitian system with extended gapless phases, *Phys. Rev. B* **106**, 054308 (2022).
- [47] J. J. Mendoza-Arenas, Dynamical quantum phase transitions in the one-dimensional extended fermi-hubbard model, *Journal of Statistical Mechanics: Theory and Experiment* **2022**, 043101 (2022).
- [48] N. Sedlmayr, P. Jaeger, M. Maiti, and J. Sirker, Bulk-boundary correspondence for dynamical phase transitions in one-dimensional topological insulators and superconductors, *Phys. Rev. B* **97**, 064304 (2018).
- [49] N. Sedlmayr, M. Fleischhauer, and J. Sirker, Fate of dynamical phase transitions at finite temperatures and in open systems, *Phys. Rev. B* **97**, 045147 (2018).
- [50] A. Khatun and S. M. Bhattacharjee, Boundaries and unphysical fixed points in dynamical quantum phase transitions, *Phys. Rev. Lett.* **123**, 160603 (2019).
- [51] K. Pöyhönen and T. Ojanen, Entanglement echo and dynamical entanglement transitions, *Phys. Rev. Res.* **3**, L042027 (2021).
- [52] C. Ding, Dynamical quantum phase transition from critical quantum quench, arXiv , 2005.08660 (2020).
- [53] A. L. Corps and A. Relaño, Theory of dynamical phase transitions in quantum systems with symmetry-breaking eigenstates, *Phys. Rev. Lett.* **130**, 100402 (2023).
- [54] S. De Nicola, A. A. Michailidis, and M. Serbyn, Entanglement and precession in two-dimensional dynamical quantum phase transitions, *Phys. Rev. B* **105**, 165149 (2022).
- [55] S. De Nicola, A. A. Michailidis, and M. Serbyn, Entanglement view of dynamical quantum phase transitions, *Phys. Rev. Lett.* **126**, 040602 (2021).
- [56] A. D. Verga, Entanglement dynamics and phase transitions of the floquet cluster spin chain, *Phys. Rev. B* **107**, 085116 (2023).
- [57] L. Rossi and F. Dolcini, Nonlinear current and dynamical quantum phase transitions in the flux-quenched su-schrieffer-heeger model, *Phys. Rev. B* **106**, 045410 (2022).
- [58] N. A. Khan, P. Wang, M. Jan, and G. Xianlong, Anomalous correlation-induced dynamical phase transitions, *Scientific Reports* **13**, 9470 (2023).
- [59] N. A. Khan, X. Wei, S. Cheng, M. Jan, and G. Xianlong, Dynamical phase transitions in dimerized lattices, *Physics Letters A* **475**, 128880 (2023).
- [60] H. Cheraghi and N. Sedlmayr, Dynamical quantum phase transitions following double quenches: persistence of the initial state vs dynamical phases, *New Journal of Physics* **25**, 103035 (2023).
- [61] L. Zhou, Q.-h. Wang, H. Wang, and J. Gong, Dynamical quantum phase transitions in non-hermitian lattices, *Phys. Rev. A* **98**, 022129 (2018).
- [62] P. Urich, N. Defenu, R. Jafari, and J. C. Halimeh, Out-of-equilibrium phase diagram of long-range superconductors, *Phys. Rev. B* **101**, 245148 (2020).
- [63] L. Zhou and Q. Du, Non-hermitian topological phases and dynamical quantum phase transitions: a generic connection, *New Journal of Physics* **23**, 063041 (2021).
- [64] U. Mishra, R. Jafari, and A. Akbari, Disordered kitaev chain with long-range pairing: Loschmidt echo revivals and dynamical phase transitions, *Journal of Physics A: Mathematical and Theoretical* **53**, 375301 (2020).
- [65] T. I. Vanhala and T. Ojanen, Theory of the loschmidt echo and dynamical quantum phase transitions in disordered fermi systems, *Phys. Rev. Res.* **5**, 033178 (2023).
- [66] D. Mondal and T. Nag, Finite-temperature dynamical quantum phase transition in a non-hermitian system, *Phys. Rev. B* **107**, 184311 (2023).
- [67] J. A. Hoyos, R. F. P. Costa, and J. C. Xavier, Disorder-induced dynamical griffiths singularities after certain quantum quenches, *Phys. Rev. B* **106**, L140201 (2022).
- [68] K. Cao, W. Li, M. Zhong, and P. Tong, Influence of weak disorder on the dynamical quantum phase transitions in the anisotropic xy chain, *Phys. Rev. B* **102**, 014207 (2020).

- [69] T. Masłowski and N. Sedlmayr, Dynamical bulk-boundary correspondence and dynamical quantum phase transitions in higher-order topological insulators, *Phys. Rev. B* **108**, 094306 (2023).
- [70] K. Wrześniewski, I. Weymann, N. Sedlmayr, and T. Domański, Dynamical quantum phase transitions in a mesoscopic superconducting system, *Phys. Rev. B* **105**, 094514 (2022).
- [71] A. L. Corps and A. Relaño, Dynamical and excited-state quantum phase transitions in collective systems, *Phys. Rev. B* **106**, 024311 (2022).
- [72] T. Masłowski and N. Sedlmayr, Quasiperiodic dynamical quantum phase transitions in multiband topological insulators and connections with entanglement entropy and fidelity susceptibility, *Phys. Rev. B* **101**, 014301 (2020).
- [73] X.-Y. Hou, Q.-C. Gao, H. Guo, and C.-C. Chien, Metamorphic dynamical quantum phase transition in double-quench processes at finite temperatures, *Phys. Rev. B* **106**, 014301 (2022).
- [74] R. Modak and D. Rakshit, Many-body dynamical phase transition in a quasiperiodic potential, *Phys. Rev. B* **103**, 224310 (2021).
- [75] Y. Zeng, B. Zhou, and S. Chen, Dynamical singularity of the rate function for quench dynamics in finite-size quantum systems, *Phys. Rev. B* **107**, 134302 (2023).
- [76] S. Stumper, M. Thoss, and J. Okamoto, Interaction-driven dynamical quantum phase transitions in a strongly correlated bosonic system, *Phys. Rev. Res.* **4**, 013002 (2022).
- [77] W. C. Yu, P. D. Sacramento, Y. C. Li, and H.-Q. Lin, Correlations and dynamical quantum phase transitions in an interacting topological insulator, *Phys. Rev. B* **104**, 085104 (2021).
- [78] V. Vijayan, L. Chotorlishvili, A. Ernst, S. S. P. Parkin, M. I. Katsnelson, and S. K. Mishra, Topological dynamical quantum phase transition in a quantum skyrmion phase, *Phys. Rev. B* **107**, L100419 (2023).
- [79] J. Z. L.-A. W. Zheng-Rong Zhu, Bin Shao, Orthogonality catastrophe and quantum speed limit for dynamical quantum phase transition, arXiv , arXiv:2308.04686 (2023).
- [80] Y.-Y. Z.-Z.-X. H. Yecheng Jing, Jian-Jun Dong, Biorthogonal dynamical quantum phase transitions in non-hermitian systems, arXiv , arXiv:2307.02993 (2023).
- [81] X.-J. Yu, Dynamical phase transition and scaling in the chiral clock potts chain, arXiv , arXiv:2309.03454 (2023).
- [82] S. M. Bhattacharjee, Complex dynamics approach to dynamical quantum phase transitions: the potts model, arXiv , arXiv:2308.14827 (2023).
- [83] A. S. D. Leela Ganesh Chandra Lakkaraju, Sudip Kumar Haldar, Predicting topological quantum phase transition via multipartite entanglement from dynamics, arXiv , arXiv:2212.13252 (2022).
- [84] S. Porta, F. Cavaliere, M. Sasseti, and N. Traverso Ziani, Topological classification of dynamical quantum phase transitions in the xy chain, *Scientific Reports* **10**, 12766 (2020).
- [85] T. Puskarov and D. Schuricht, Time evolution during and after finite-time quantum quenches in the transverse-field Ising chain, *SciPost Phys.* **1**, 003 (2016).
- [86] C. Karrasch and D. Schuricht, Dynamical quantum phase transitions in the quantum potts chain, *Phys. Rev. B* **95**, 075143 (2017).
- [87] S. Zamani, R. Jafari, and A. Langari, Floquet dynamical quantum phase transition in the extended xy model: Nonadiabatic to adiabatic topological transition, *Phys. Rev. B* **102**, 144306 (2020).
- [88] A. Kosior and K. Sacha, Dynamical quantum phase transitions in discrete time crystals, *Phys. Rev. A* **97**, 053621 (2018).
- [89] R. Jafari and A. Akbari, Floquet dynamical phase transition and entanglement spectrum, *Phys. Rev. A* **103**, 012204 (2021).
- [90] A. Kosior, A. Syrwid, and K. Sacha, Dynamical quantum phase transitions in systems with broken continuous time and space translation symmetries, *Phys. Rev. A* **98**, 023612 (2018).
- [91] J. Najji, M. Jafari, R. Jafari, and A. Akbari, Dissipative floquet dynamical quantum phase transition, *Phys. Rev. A* **105**, 022220 (2022).
- [92] R. Jafari, A. Akbari, U. Mishra, and H. Johannesson, Floquet dynamical quantum phase transitions under synchronized periodic driving, *Phys. Rev. B* **105**, 094311 (2022).
- [93] J. , R. Jafari, L. Zhou, and A. Langari, Engineering floquet dynamical quantum phase transitions, *Phys. Rev. B* **106**, 094314 (2022).
- [94] J. C. Budich and M. Heyl, Dynamical topological order parameters far from equilibrium, *Phys. Rev. B* **93**, 085416 (2016).
- [95] K. Cao, S. Yang, Y. Hu, and G. Yang, Dynamics of the geometric phase in inhomogeneous quantum spin chains, *Phys. Rev. B* **108**, 024201 (2023).
- [96] K. Sim, R. Chitra, and P. Molignini, Quench dynamics and scaling laws in topological nodal loop semimetals, *Phys. Rev. B* **106**, 224302 (2022).
- [97] S. Bhattacharjee and A. Dutta, Dynamical quantum phase transitions in extended transverse ising models, *Phys. Rev. B* **97**, 134306 (2018).
- [98] A. Dutta and A. Dutta, Probing the role of long-range interactions in the dynamics of a long-range kitaev chain, *Phys. Rev. B* **96**, 125113 (2017).
- [99] S. Sharma, A. Russomanno, G. E. Santoro, and A. Dutta, Loschmidt echo and dynamical fidelity in periodically driven quantum systems, *Europhysics Letters* **106**, 67003 (2014).
- [100] X. Nie, B.-B. Wei, X. Chen, Z. Zhang, X. Zhao, C. Qiu, Y. Tian, Y. Ji, T. Xin, D. Lu, and J. Li, Experimental observation of equilibrium and dynamical quantum phase transitions via out-of-time-ordered correlators, *Phys. Rev. Lett.* **124**, 250601 (2020).
- [101] T. Tian, H.-X. Yang, L.-Y. Qiu, H.-Y. Liang, Y.-B. Yang, Y. Xu, and L.-M. Duan, Observation of dynamical quantum phase transitions with correspondence in an excited state phase diagram, *Phys. Rev. Lett.* **124**, 043001 (2020).

- [102] F. J. González, A. Norambuena, and R. Coto, Dynamical quantum phase transition in diamond: Applications in quantum metrology, *Phys. Rev. B* **106**, 014313 (2022).
- [103] R. Shen, T. Chen, M. M. Aliyu, F. Qin, Y. Zhong, H. Loh, and C. H. Lee, Proposal for observing yang-lee criticality in rydberg atomic arrays, *Phys. Rev. Lett.* **131**, 080403 (2023).
- [104] J. Marino and A. Silva, Relaxation, prethermalization, and diffusion in a noisy quantum ising chain, *Phys. Rev. B* **86**, 060408 (2012).
- [105] J. Marino and A. Silva, Nonequilibrium dynamics of a noisy quantum ising chain: Statistics of work and prethermalization after a sudden quench of the transverse field, *Phys. Rev. B* **89**, 024303 (2014).
- [106] U. Divakaran, S. Sharma, and A. Dutta, Tuning the presence of dynamical phase transitions in a generalized  $xy$  spin chain, *Phys. Rev. E* **93**, 052133 (2016).
- [107] S. Sharma, U. Divakaran, A. Polkovnikov, and A. Dutta, Slow quenches in a quantum ising chain: Dynamical phase transitions and topology, *Phys. Rev. B* **93**, 144306 (2016).
- [108] B. Dóra, F. Pollmann, J. Fortágh, and G. Zaránd, Loschmidt echo and the many-body orthogonality catastrophe in a qubit-coupled luttinger liquid, *Phys. Rev. Lett.* **111**, 046402 (2013).
- [109] U. Bhattacharya and A. Dutta, Emergent topology and dynamical quantum phase transitions in two-dimensional closed quantum systems, *Phys. Rev. B* **96**, 014302 (2017).
- [110] U. Bhattacharya, S. Bandyopadhyay, and A. Dutta, Mixed state dynamical quantum phase transitions, *Phys. Rev. B* **96**, 180303 (2017).
- [111] R. Jafari, Thermodynamic properties of the one-dimensional extended quantum compass model in the presence of a transverse field, *The European Physical Journal B* **85**, 167 (2016).
- [112] K. Takahashi, Quantum lower and upper speed limits using reference evolutions, *New Journal of Physics* **24**, 065004 (2022).
- [113] M. V. Berry, Geometric amplitude factors in adiabatic quantum transitions, *Proceedings of the Royal Society of London. Series A: Mathematical and Physical Sciences* **430**, 405 (1990).
- [114] D. Bouwmeester, G. P. Karman, C. A. Schrama, and J. P. Woerdman, Observation of interference in transitions due to local geometric phases, *Phys. Rev. A* **53**, 985 (1996).
- [115] D. Bouwmeester, G. P. Karman, N. H. Dekker, C. A. Schrama, and J. P. Woerdman, Observation of the geometric amplitude factor in an optical system, *Journal of Modern Optics* **43**, 2087 (1996).
- [116] G. Szegő, A. erdélyi, w. magnus, f. oberhettinger and fg tricomi, higher transcendental functions, *Bulletin of the American Mathematical Society* **60**, 405 (1954).
- [117] M. Abramowitz, I. A. Stegun, and R. H. Romer, *Handbook of mathematical functions with formulas, graphs, and mathematical tables* (1988).
- [118] K. Mullen, E. Ben-Jacob, Y. Gefen, and Z. Schuss, Time of zener tunneling, *Phys. Rev. Lett.* **62**, 2543 (1989).
- [119] J. Dziarmaga, Dynamics of a quantum phase transition: Exact solution of the quantum ising model, *Phys. Rev. Lett.* **95**, 245701 (2005).
- [120] M. Heyl, Scaling and universality at dynamical quantum phase transitions, *Phys. Rev. Lett.* **115**, 140602 (2015).
- [121] N. V. Vitanov and B. M. Garraway, Landau-zener model: Effects of finite coupling duration, *Phys. Rev. A* **53**, 4288 (1996).
- [122] N. V. Vitanov, Transition times in the landau-zener model, *Phys. Rev. A* **59**, 988 (1999).